Advances in Industrial and Manufacturing Engineering 8 (2024) 100137

Contents lists available at ScienceDirect

Advances in Industrial and Manufacturing Engineering

journal homepage: www.sciencedirect.com/journal/advances-in-industrial-and-manufacturing-engineering

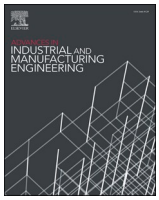

Experimental and analytical ways of finding the function of the maximum accumulated damage under operating modes with overloads

S. Belodedenko [a], O. Hrechanyi [b,*], V. Hanush [a], Y. Izhevskyi [a]

[a] Department of Industrial Machinery Engineering, Ukrainian State University of Science and Technologies, Dnipro, Ukraine
[b] Department of Metallurgical Equipment, Zaporizhzhia National University, Zaporizhzhia, Ukraine

ARTICLE INFO

Keywords:
Overload
Loading history
Accumulated damage

ABSTRACT

The problem of overloading was characterized as a factor of load history in the modern resource assessment methodology. The signs by which a loading cycle can be considered an overload were defined. A correlation was obtained between the failure mechanics approach and the damage accumulation approach to survivability prediction. An experimental and analytical method of its adjustment has been developed based on the regularities of the impact of loads on the accumulated damage. Its use in obtaining models of damage accumulation in 40Cr and 35CrMnSi steels was shown. New experimental data were obtained on the behavior of the accumulated damage function in the stress localization zones during bending, and an explanation of its non-monotonicity under the influence of operational factors was found.

1. Introduction

In the second half of the 20th century damage summation laws cultivation were popular among fatigue experts. They allowed us to consider the non-stationary loading factor in predicting fatigue durability. On the other side, this attention was driven by the use of S–N models (fatigue curves) where elementary (per 1 cycle) damage d_i is related to relative durability N_i: $d_i = 1/N_i$. Then, the number of cycles at various load levels to the limit state (cumulative durability) NVA would be determined by the law of damage summation. According to Miner's rule, the current damage is determined as the sum $D = \Sigma(n_i/N_i)$ (Miner, 1945). At the time of reaching the limit state of the material (appearance of cracks, failure), the current damage transforms into the accumulated limit damage $a_0 = \Sigma n_i d_i$. In general, the marginal accumulated damage a0 is a function of the set. For modeling reasons, it is simplified to a function that depends on certain indicators of the X_i, mode, which determine the shape of the load block. Therefore, by using accumulated limit damage as a function of $a_0(X_i)$, one can express $\Sigma n_i d_i = a_0(X_i)$.

The diversity of damage summation laws is explained by the absence of physical meaning in the d_i factors, complicating the determination of the boundary value of cumulative damage. On the other side, in prediction, it was customary to consider all possible operating conditions, resulting in overly broad load distribution populations (spectra) that acted over fairly long periods of equipment operation. Such characteristic periods could range from one year to the entire total equipment service life. Along with the high sensitivity of fatigue strength criteria to non-stationary load factors, the consequence of such forecasting was an unsatisfactory correspondence of their results to actual operational lifetimes. This necessitated, at that stage of technological development, certain adjustments to universal damage summation laws and the creation of new ones. In the comprehensive review by Fatemi-Yang, more than 50 damage accumulation models that existed by the end of the 20th century are listed (Fatemi and Yang, 1998).

Currently, the severity of this problem has somewhat diminished due to the following circumstances. Firstly, modeling loading as random processes, using the load history method, allows for a more defined approach to this stage of prediction compared to the spectral method. Reducing the degree of uncertainty leads to greater forecast relevance (Liu and Mahadevan, 2007; Będkowski, 2014; Abdullah et al., 2006; Nottebaere et al., 2017). Secondly, the widespread implementation of automated load monitoring tools during operation contributes to this as well (Chan et al., 1999; Krot et al., 2020; Garcia et al., 2022). Thirdly, modern fatigue criteria (e.g., energy-based) are less sensitive to non-stationary load factors. Therefore, models obtained under stationary conditions can be used, although there are certain limitations (Abdullah et al., 2006; Nottebaere et al., 2017; Santecchia et al., 2016; Fomichev, 2006). Finally, the availability of technical diagnostic tools for a wide range of mechanical systems allows for timely detection of fatigue cracks (Lee et al., 2022). After this, the problem of damage

* Corresponding author.
E-mail address: hrechanyi@znu.edu.ua (O. Hrechanyi).

https://doi.org/10.1016/j.aime.2024.100137
Received 15 November 2023; Received in revised form 29 January 2024; Accepted 2 February 2024
Available online 10 February 2024

Abbreviations

D	current accumulated fatigue damage over n load cycles
di	elemental damage for 1 load cycle of the i level
a_{0j}	internal block ultimate damage obtained under conditions of regular loading by the j form block
a_r	internal block marginal damage obtained under conditions of randomized loading with blocks of different shapes
i	block load level number
Xi	load indicator of the i-th level of the block
j	number of loading unit λ
B i OL	the main and overload levels of the block, which are used instead of the number and in the developed load model
n_i	the number of load cycles of the i level of the block
c_i	the relative number of load cycles of the i block level in the total number of block cycles nλ
$a_0(X_i)$	accumulated limit damage function
α_σ	theoretical stress concentration factor
FCGR	fatigue crack growth rate
R_{0L}	cycle asymmetry coefficients
n_{OL}	number of cycles
c_{OL}	relative duration of the overload action
SIF	stress intensity factor
LDR	linear damage rule
HCF	high-cycle fatigue zone
LCF	low-cycle fatigue zone

summation transitions into the problem of determining the rate of failure under operational loading. The concept of crack growth has gained widespread acceptance since cracks are directly related to damage (Fatemi and Yang, 1998).

Despite the mentioned circumstances, the development of new damage accumulation models continues. This is evident from a recent review of this problem (Hectors et al., 2021), which includes works conducted over the past 20 years. There is a trend towards creating nonlinear damage accumulation models that reflect their kinetics during operation. It has been concluded that the majority of available fatigue damage models are validated only for relatively small sets of experimental data, making it difficult to assess their general applicability. Miner's rule still remains the most widely used approach for fatigue design under variable amplitude loading and has been incorporated into leading design standards for steel structures (Hectors et al., 2021).

One of the directions where research on damage accumulation remains relevant is in operating conditions with overloads. While the impact of overloads on the fatigue life of most metals can be considered and understood, similar investigations are not yet concluded for composite materials, additively manufactured products, welded, and bonded joints (Sonsino et al., 2011; Hesseler et al., 2021; Zhang and Wei, 2022a; Sousa et al., 2022; Bleicher et al., 2019).

In cases of overloads, there is an anomaly in the behavior of the $a_0(X_i)$ function. This anomaly is characterized by its non-monotonicity and the presence of extrema. Known damage accumulation models, including nonlinear ones, often fail to predict the durability of systems under overload conditions. So, overload means such a level of emission, after which the intensity of damage accumulation or the rate of crack growth changes. Hence the signs of overload. First, from the standpoint of external influence on the element of the mechanical system, this is a load level with a low frequency of occurrence. For the load model in the form of blocks, the frequency of occurrence embodies relative duration of action of the c_{OL} overload level. Therefore, the first formal sign of overload is $c_{OL} \leq 0.01$–0.02 (Belodedenko, 2010; Belodedenko et al., 2022). Secondly, from the point of view of the internal resistance of the element, such an overload should be sufficient to create local plastic deformations. They appear in zones of stress concentration or at the top of a crack. After that, the mode of cyclic deformation changes.

The fundamental principles of constructing the $a_0(X_i)$ function under conditions of regular overloads were outlined by the authors in the article (Belodedenko et al., 2020). However, that article lacks substantive justification of the model, pathways to its resolution, and implementation results. The purpose of this research was to develop an engineering model of the limit accumulated damage for overload conditions and a method (algorithm) for obtaining it.

The objectives of the study included:

- Establishing a connection between the fracture mechanics approach and the damage accumulation approach in predicting durability.
- Reviewing the latest developments and trends in studying the influence of overloads on crack growth.
- Identifying the primary factors influencing the adjustment of the damage accumulation function for overload conditions.
- Experimentally verifying the models and demonstrating the method of obtaining them based on the results of software testing with a minimal number of modes.
- Demonstrating the application of the model in equipment maintenance.

2. Materials and methods

For model verification, high-strength steels 40 Cr (equivalent to AISI 5140) and 35 CrMnSi (equivalent to PN 35HGSA) were chosen. Test specimens for concentrated bending tests were fabricated from stampings of cutter holders for coal combines. Rods measuring 35 mm in diameter and 120 mm in length were used as stock material. After heating, they were flattened into flat bars using a press with a single force of 10 MN, and these bars were subsequently subjected to mechanical and thermal processing. Normalization followed by isothermal quenching was used for this purpose. The achieved levels of hardness (HRC), ultimate strength σ_U, and cyclic fracture toughness K_{fc} are presented in Table 1.

Unnotched and notched specimens had a length of 136 mm, a section height of 27 mm, and a width of 15 mm (Fig. 1). In the middle of the notched sample, under the spot of application of the load on the stretched side of the beam, there was a U-shaped cut 2 mm wide, 5 mm deep, with a nominal rounded radius of 1 mm.

This notch created a theoretical stress concentration factor of $\alpha_\sigma = 3.5$. A notch for crack initiation was created using an abrasive wheel after heat treatment.

The tests were conducted with cycle asymmetry coefficients $R_{0L} = R_B = 0.10$ to 0.15 at a frequency of 7.5–12.5 Hz (main stage B) and 1–3 Hz (overloads OL). The number of cycles at the overload level was $n_{OL} = 200$, and the relative duration of the action was $c_{OL} = 0.01$.

Table 1
Mechanical properties of the steels, as well as fatigue life curve parameters for maximum cycle stress in MPa.

#	steel	HRC	σ_U	Parameters of Eq. (1)				K_{fc}, MPa·m$^{1/2}$
				$\alpha_\sigma = 1$		$\alpha_\sigma = 3.5$		
				m	B	m	B	
1	40 Cr	51	1760	6.5	24.4	6.0	20.7	49
2	35 CrMnSi	43	1500	9.4	32.7	8.8	27.6	113

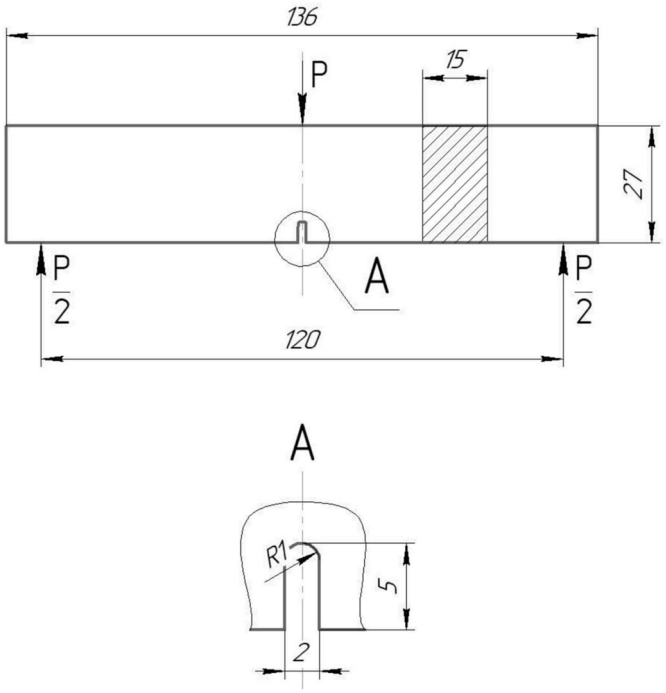

Fig. 1. Scheme of the sample and tests.

3. Theory

3.1. The relationship between fracture mechanics and damage accumulation approaches

Earlier, the authors noted the similarity between the processes of accumulating damage up to the limit state, denoted as a_0, and the fatigue crack growth rate (FCGR) under the influence of non-stationary overloading conditions (Belodedenko, 2010). Although according to conventional concepts, each of these indicators is used for different stages of fatigue failure, this similarity suggests that both cases involve a single crack development process. This provides a basis for applying Miner's rule in crack growth (fatigue life) models. This approach was used by Fleck, who compared FCGR under periodic underloads and overloads with FCGR predicted by linear damage accumulation (Fleck, 1985). Subsequently, the fundamental assumption of this approach was confirmed, which is that both crack initiation and crack growth are governed by the same fatigue damage mechanism (Ding et al., 2017). In other words, under overloads, early crack formation is observed (especially in stress localization zones), and in certain cases, the durability at the crack initiation stage can be neglected, as it is governed by the same fatigue damage mechanism. Based on this, a fatigue crack growth method was developed in which the number of cycles required for a crack to reach a critical size under non-stationary conditions is determined using the parameter a_0. In this method, the function of accumulated damage as a function of the loading parameters, denoted as $a_0(X_i)$, is obtained through computational testing on fatigue specimens (Belodedenko et al., 2006). Since these tests are designed to determine fatigue resistance, they exhibit a uniform stress state, making it difficult to observe crack development. Under such conditions, during cyclic tests under axial loading of cylindrical specimens made of aluminum alloys and high-strength steels, peculiarities of the influence of overloading process parameters X_i on damage accumulation were established (Belodedenko et al., 1997, 2006).

The most comprehensive information about the influence of non-stationary overloading processes on durability is provided by fatigue tests of specimens designed to determine resistance to failure. Through these tests, kinetic fatigue crack growth diagrams can be obtained, which represent the dependency between the FCGR, denoted as V, and the SIF. However, directly using such a diagram to predict the durability of real structures can cause difficulties. This is mainly due to the fact that cracks appear in hard-to-reach places (e.g., joints), and their geometry is often unknown.

Therefore, a model has been developed to determine the equivalent FCGR under non-stationary loading conditions, denoted as V_{VA}, which is related to the FCGR under stationary loading conditions, denoted as V_{CA}, through a proportionality coefficient g: $V_{VA} = g \cdot V_{CA}$. Analogous to fatigue curves, representing durability as the period of crack growth from the initial size to the critical size N_g, the fatigue life curves can be described by the equation (Belodedenko et al., 2022):

$$N_g \cdot \sigma^m = 10^B. \quad (1)$$

The parameters m and B are derived from the statistical analysis of the results of cyclic tests under stationary loading with stress σ. Considering this, the fatigue life in Eq. (1) can be denoted as N_{CA}. For the block model of non-stationary loading, where the parameters are the stress level σ_i and its relative duration c_i, the equivalent stress for the block will be (Belodedenko, 2003):

$$\sigma_e = \left(\sum \sigma_i^m \cdot c_i\right)^{\frac{1}{m}} \cdot a_0^{\frac{-1}{m}}. \quad (2)$$

If this stress is substituted into (1), it can provide the number of cycles at different levels for crack growth to a critical size, which is the fatigue life under variable amplitude loading, denoted as N_{VA}. The equivalence of both approaches is confirmed by relationships (Belodedenko, 2003):

$$a_0 = N_{VA}/N_{CA} = V_{CA}/V_{VA} = 1/g. \quad (3)$$

When regular overloads appear, the variables take on values – $g < 1$, $a_0 > 1$. In other words, the fatigue FCGR under variable amplitude loading denoted as V_{VA}, decreases relative to the FCGR under stationary background loading, denoted as V_{CA}.

3.2. The influence of overloads on the fatigue crack growth process

The effect of crack growth retardation after overloads has been known for 50 years. Its discovery is associated with the names Rice, Stephens, and Jones (Salvati et al., 2017; Rice and Stephens, 1973; Jones, 1973). The main reason for the overload effect can be considered as the plasticity of the crack front. At high local deformations around the plastic zone, a compressive residual stress field forms, which slows down the FCGR. Additionally, the plasticity of the crack front influences phenomena such as crack closure and blunting (Borrego et al., 2005). Along with the crack interaction mechanism and the complication of their trajectories, these phenomena are also considered among the causes. However, there has been no clear consensus on the significance of these mechanisms (Salvati et al., 2017).

When predicting fatigue life under overload conditions, two widely used models are the Wheeler model and the Willenborg model. In these models, the value of the proportionality coefficient g is determined by the relationship between the zones of failure from overload and the main background (Wheeler model) or by the ratio of nominal and effective SIF (Willenborg model). There are many versions of these models, and they are used for fatigue life prediction through FCGR monitoring (Pereira et al., 2007). In recent years, new modifications of these models have been proposed, which more accurately consider the shape of the failure zone (Cai et al., 2022; Shakeri et al., 2021).

This approach is mainly used by researchers to interpret the results of fatigue tests. The kinetic models built on these principles do not fully reflect the complexity of the underlying processes. They do not take into account the possibility of an increase in the FCGR when varying the load amplitude, even though when studying the effect of overloads acting in the background of the main loading process, it has been found that the change in the g coefficient is non-monotonic, with extreme values

(Phillips, 1999). This non-monotonic behavior may be associated with the absence of the crack closure effect, which is observed when the overload stress exceeds the yield strength (Zhang and Wei, 2022b). In such cases, as the overload increases, the degree of closure decreases, reducing the inhibiting effect. Overloads affect short and long cracks differently: in bending conditions, short cracks show an increase in FCGR, while for long cracks, FCGR decreases (Song et al., 2001). Therefore, not only the relative magnitude of the overload matters but also the stage of crack development, which is influenced by the level of loading in the main process.

The new push in studying FCGR under variable amplitudes was associated with the discovery of an acceleration of FCGR after overloading in compression (Fleck, 1985). This type of extreme loading, where the minimum stress of the cycle becomes less than the minimum stress of the background cycle, is called underloading. The reasons for the increase in FCGR after underloading may be related to the appearance of residual tensile stresses and the smoothing of the fracture surface, which reduces the degree of crack closure (Field et al., 2022). The loss of crack closure capability does not contribute to the inhibition of FCGR (Zhang and Wei, 2022b). Similar to overloads, underloads affect short and long cracks differently: it has been established that short cracks accelerate the most (Field et al., 2022). In fact, studying underload conditions corresponds to investigating the influence of the cycle asymmetry factor. Compression overloads induce local tensile residual stresses ahead of the crack tip. These local tensile residual stresses locally increase the cycle asymmetry factor R, leading to an increase in FCGR and a decrease in the value of a_0 (Zhou et al., 2015).

Another current research direction related to crack arrest is the study of mixed-mode fracture. Overloads in a mixed mode I + II tend to inhibit FCGR but to a lesser extent than pure mode I overload. There are indications of a negative influence of mode II. Its contribution adds to FCGR both at the overload and background levels, as the crack tip becomes sharper (Shakeri et al., 2021; Rege et al., 2019; Xie et al., 2022). For welded joints, research on the influence of structural thickness on the inhibitory effect during overloads is relevant (Gadallah et al., 2023). Thanks to the application of modern research methods, such as neutron diffraction, it has been clarified that tension overloads create a slightly larger zone of compressive residual stresses than previously believed. Significantly larger compressive stresses remain on the surface than in the thickness (Seo et al., 2017).

Indeed, according to conventional wisdom, underloads tend to accelerate FCGR, while overloads tend to inhibit it (Rege et al., 2019). This latter observation provides a basis for developing methods to extend the service life of damaged structures. This can be achieved through artificially induced and controlled overloads (Tipton et al., 1999; Zhang et al., 1998).

Separately, the influence of the type of sequence of load levels should be considered. As it is known, increasing blocks of load are classified, where low levels are ahead of high levels (L–H), also decreasing blocks where high levels are ahead of low levels (H–L). Miner's rule does not consider sequence type, the kinetics of damage accumulation d deviates from linear. For H–L loads, damage accumulates more intensively than with L–H blocks. If for a stationary loading the value $a_{0CA} = 1$, then for H–L blocks it can be considered $a_{0\,H-L} \to 0.5$, and for L–H blocks $a_{0L-H} \to 1.5$. Such conclusions follow from the test results of titanium alloy samples (Lin et al., 2018). A similar situation is observed for steel and aluminum alloy samples (Peng et al., 2015). But it should be noted that the test results for L–H and H–L blocks are included in the interval of natural dispersion of durability under stationary loading.

The reverse pattern is observed at the stage of crack growth. H–L blocks definitely inhibit the development of cracks, contributing to increase survivability (Neto et al., 2022; Laseure et al., 2015). However, for L–H blocks, such inhibition is less pronounced (Neto et al., 2022). Even on the contrary, FCGR can accelerate (Laseure et al., 2015). Such fears are related to the fact that overload will behave like underload. A similar situation is typical for a very small number of blocks before destruction. With periodic overloads and a high "shuffling" of blocks, the Sequence effect decreases. Fundamentally, this effect of load history on FCGR has not been fully studied (Neto et al., 2022). The behavior of the crack is largely influenced by which mechanism of its inhibition is dominant. For example, the difference in impact between H–L and L–H loading is explained by the crack closing phenomenon (Neto et al., 2022).

In recent years, due to the popularization of the Internet and increased computer processing power, machine learning methods have gained widespread use. They are employed for predicting fatigue life, including in the presence of overload conditions (Zhang and Wei, 2022a, b; Bleicher et al., 2019; Duan et al., 2023). This is a powerful and promising approach that provides a high level of accuracy in predicting results consistent with actual outcomes. Among its drawbacks are the cost associated with it and the need for a large amount of training data (Bleicher et al., 2019). The latter limitation can be overcome by collecting test results (Duan et al., 2023). In this regard, labor-intensive tests, which will be presented later, can be of interest.

3.3. The model for adjusting accumulated damage

3.3.1. Modeling operational loading for modes with overloads

With purely random loading, there is no periodicity, which is not typical for technological equipment. The established work performance technology makes the loading process pseudo-random, and the established drive frequency characterizes the operational process periodically-random (Peng et al., 2015). Therefore, they can be schematized with formalized blocks reflecting the loading history.

The operation of most mining and metallurgical complex machinery is characterized by the occurrence of random overloads that occur against the background of normal loading conditions. The appearance of overloads usually happens when technical operation rules are violated, although there are objective prerequisites for this. The fundamental principles of modeling processes with overloads were developed with the participation of one of the authors at the beginning of the 21st century (Belodedenko, 2003; Collacott, 1985).

A real random process is represented as a basic (background, sometimes baseline) process B and a sequence of outliers OL (Fig. 2). The sequence of outliers (overloads) of different levels divides the basic process into blocks λ_j. According to the concepts of fatigue resistance experts, any loading history can be represented as a sequence of overloads and underloads (Rege et al., 2019). The duration of one block $n_\lambda = n_B + n_{OL}$ is determined by the period between the outliers, and the frequency of outliers can be determined from the periodicity diagram of emissions, which was developed by the authors (Belodedenko, 2003). According to it, the number of cycles at the base level n_B is determined depending on the relative level of overload or its peak factor. The number of n_{OL} cycles is determined from the ratio $c_{OL} = n_{OL}/n_\lambda$ assuming a certain relative duration of the overload from the condition $c_{OL} \le 0.01$.

Thus, the loading is represented as a sequence of two-level blocks (Fig. 1). The parameters of the loading levels B and OL include elementary damage d_i, the number of loading cycles n_i, and the asymmetry coefficient of the cycle (stress ratio) R_i. The mode of overloading and/or underloading is modeled based on the value of R_i. The level of loading is also characterized by its frequency and the coefficients of damage variation and asymmetry.

3.3.2. The influence of overloads on accumulated damage

If the critical damage in the equation $a_0 = \Sigma n_i d_i = 1$ is equal to one, then the linear damage rule (LDR) is observed, where the damage from each stage is proportional to the load history on it. In general, LDR for non-stationary modes is considered a hypothesis that needs to be experimentally confirmed. In the general case, it is necessary to adjust either the damage rate or the accumulated damage.

The possibility of using LDR relies on treating accumulated damage as a random variable. Indeed, when correctly defining fatigue curve

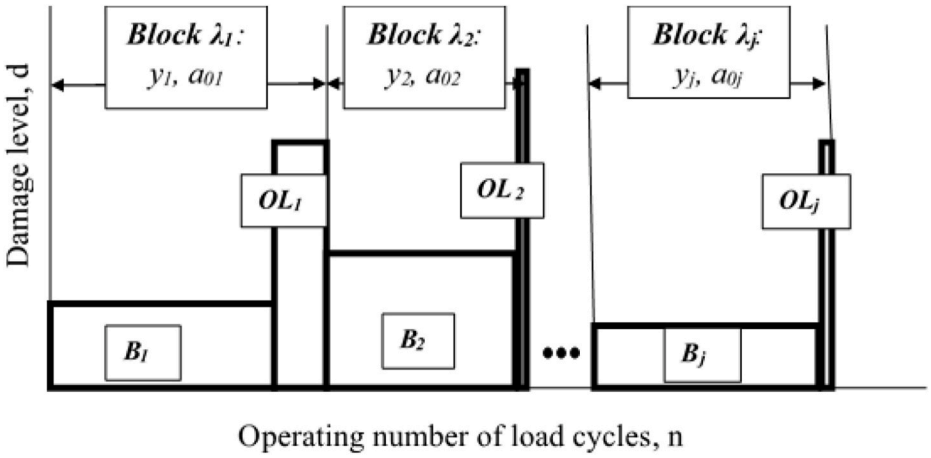

Fig. 2. Schematization of operational loading with overload levels in blocks.

parameters for most types of loading conditions, the value a0 is distributed in the range from 0.1 to 2.0 with an expected value of $a_0 = 1$. However, the situation is compounded by the fact that in a formal approach to calculations, the value a0 can change within wider limits than mentioned above. Similar situations are encountered in loading processes with a wide variation in parameters, where rare spikes - overloads - can take on significant values. In such a situation, interpreting accumulated damage as a random variable is unacceptable. This leads to underestimated guaranteed durability predictions. At the same time, identifying the deterministic component in factors that are treated as random is a fundamental principle for improving safety in the step-by-step assignment of resources.

The main characteristic of overloads is their low frequency of occurrence: $c_{OL} \leq 0.01$. Overloads are dangerous not so much because of the damage they directly cause, but because of the poorly predictable subsequent intensity of its accumulation. The non-stationary loading factor significantly affects the LDR hypothesis when the number of blocks is less than 20, and the loading history factor when the number of blocks is less than 10 (Belodedenko et al., 1997). This number of blocks in operation is due to rare spikes. As a result, the actual loading process is naturally divided into blocks by means of spikes - overloads. For processes that can be schematized in this way, a methodology has been developed to search for fatigue distribution functions, where their expected value is determined as (Belodedenko, 2005):

$$N_{VA0} = a_r \cdot \sum_{\lambda_1}^{\lambda_j} a_{0j} \cdot y_j^{-1}, \quad (4)$$

where a_r – interblock accumulated damage, taking into account the random nature of the process; a_{0j} – intrablock accumulated damage for the j-th form, taking into account the non-stationarity of the load; $y_i = c_i \bullet d_i$ – the damaging characteristic of the j-th form block.

It is evident that a key role here is assigned to the value of a_0, which is adjusted depending on the parameters of the schematized block. An anomaly in the effect of rare load spikes on the damage accumulation process has been identified. This anomaly is not only characterized by a significant deviation of the value of a_0 from unity but also by a disruption of the self-similarity of the damage kinetics, which complicates their monitoring. In practice, non-self-similarity is taken into account by adjusting the fatigue damage (Gusev, 1989).

As previously noted, the main characteristic of the function $a_0(X_i)$ is its non-monotonic behavior depending on the key factors. For instance, the relative duration of overload results in a minimum of the function a_0 in the range of $c_{OL} = 0.01 \ldots 0.001$ (Belodedenko, 2005; Shlyushenkov and Tatarintsev, 1994). However, if the maximum overload stress is high and the nature of the failure changes, this extremum is not observed. Therefore, the second characteristic of the function $a_0(X_i)$ is the interaction of factors (Belodedenko et al., 2023). Such behavior is well described by polynomial models, the technique for obtaining which is based on software testing with two-stage blocks according to second-order experiment plans (Belodedenko et al., 1997, 2006; Belodedenko, 2003). A set of significant factors has been identified, including the overload stress ratio, the relative magnitude of the background or baseline process B, and their cycle asymmetry coefficients. Defining overload as a stage with a relative duration of less than 1% reduces the number of influencing factors. The possibility of applying polynomial models of accumulated damage a_0 has been tested for loading parameters expressed in terms of force and deformation criteria under tension-compression and cyclic bending conditions, for fatigue crack initiation and propagation periods (Belodedenko et al., 1997; Gusev, 1989). The identical behavior of the found a_0 functions served as the basis for expressing loading parameters directly in terms of damage d or their logarithms lg$d$, making the model universal (Belodedenko et al., 1997, 2006; Belodedenko, 2003).

Overloads, by affecting stress localization zones, create elastoplastic deformations that, in conditions of non-uniform stress-strain states, leave stresses of the opposite sign to external stresses after unloading. Subsequent deformation processes will occur with a different cycle asymmetry than the asymmetry of the external load. This internal non-stationarity explains the effect of the loading history factor. Tensile overloads, as a rule, increase durability. During the crack initiation stage, this is associated with a reduction in the cycle asymmetry on the main stage, and during the fracture development stage, it is related to residual compressive stresses in front of the crack tip. Alternating sign overloads neutralize the discussed effects of fracture retardation. This phenomenon was initially formulated for aluminum alloy 2024-T3 under single overloads during the crack growth stage (Dawicke, 1997), and for aluminum alloy 01570 M under sequential overloads during the crack initiation stage (Belodedenko et al., 1997). Subsequently, similar behavior was observed in structural steels (Belodedenko et al., 2006). This phenomenon is explained by the fact that elastoplastic compressive deformations remove the previously favorable residual stresses, and, conversely, negative tensile residual stresses appear. Additionally, crack opening stresses decrease, and the effective stress intensity factor increases. Therefore, the cycle asymmetry factor for overload conditions is considered one of the most significant factors, but it is often ignored in calculations based on energy criteria, which have not been validated by targeted experiments.

The influence of cycle asymmetry, R_{OL}, and the main process, R_B, was extensively studied for high-strength steels characterized by such loading conditions (Belodedenko et al., 2006). Confirming the general trend of an increase in the a_0 value with increasing cycle asymmetry, the

main result of these studies is the variability in the degree of influence of cycle asymmetry depending on the damage level of the stage. The cycle asymmetry factor has a more significant impact than the asymmetry factor of the main process.

In stress concentration zones, an increase in the value of a_0 is observed compared to areas with a weak stress gradient. This feature has been identified, including for symmetric cycles. Therefore, it is not related to the internal nonstationarity of loading (Belodedenko et al., 1997). However, convincing explanations have not been provided. At the same time, it has been noted that similar patterns apply during the accumulation of scattered fatigue damage and crack growth under overload conditions. However, mechanics of fracture models are not widely applied to equipment in the mining and metallurgical complex for several reasons. Predicting the lifespan based on accumulated damage remains the prevailing method in engineering practice. The polynomial models under consideration have drawbacks: the lack of physical meaning in regression coefficients and the labor-intensive experimental determination of these coefficients. To obtain a two-factor model, it is necessary to conduct seven experiments with several samples in each, not counting tests in stationary mode.

Considering the above, the refined goal of this research was to develop an engineering method for obtaining a damage accumulation correction model under overload conditions that would be less labor-intensive compared to the polynomial model approach but would also reflect the patterns of influence of key loading parameters, similar to the latter.

3.3.3. The correction model

In order to analytically obtain the damage accumulation model, it is necessary to consider the influence of each factor separately, representing it in the form of:

$$a_0(X) = a_0(X_{OL}; X_B; R) = a_{0L} + \Delta a_B + \Delta a_R, \quad (5)$$

where: $a_{OL} = a_0(X_{OL})$ – basic function a_0;

Δa_B – adjustment of the basic function due to the influence of factor X_B;

Δa_R – adjustment of the basic function based on the influence of cycle asymmetry.

In this model, the value of the *OL* and *B* levels is characterized not by the elementary damages d_{OL} and d_B, but by their relative values X_{OL} and X_B. Then $X_{OL} = d_{OL}/d_B$, $X_B = d_B/d_{Bmin}$. The minimum value of accumulated damage a_{0min} corresponds to the main level B with elemental damage d_{Bmin}. Usually, this value corresponds to the limit of endurance, and in this case $d_{Bmin} = 10^{-7}$ is taken, which gives $X_B = d_B \times 10^7$.

In natural coordinates, $a_0 - X_{OL}$, the basic function $a_0(X_{OL})$ has a concave shape (1, Fig. 2) with a minimum a_{0min} in the range from $X_{OL0} = 10$ (steels) to $X_{OL0} = 100$ (aluminum alloys). The smallest values of the a_{OL} function, $a_{OL} = a_0(X_{OL})$, are observed with parameters $R = -1$ and $X_B = 1$ ….5, reaching average values of $a_{0min} = 0.5$ (steels) and $a_{0min} = 0.3$ (aluminum alloys). Let's represent the a_{OL} function as descending and ascending branches with a common point at coordinates (X_{OL0}; a_{0min}). The presence of a descending branch is characteristic of alternating sign modes ($R < 0$) and can be explained as follows. The graph of the $a_0(X_{OL})$ function starts from the point $X_{OL} = 1$, $a_0 = 1$, which corresponds to the stationary mode. When there are minor overloads ($X_{OL} < X_{OL0}$), firstly, a macrocrack forms over a significant period of time, and the overall durability *N* almost does not contain the fatigue life period N_g. The decrease in the value of a_0 is due to the nonstationarity factor (Influence of VA zone, Fig. 3).

Such loading represents a complex of degradation processes in which the damage accumulation rate increases compared to the base stationary process. Secondly, small overloads cannot effectively arrest the growth of a crack, especially if part of the cycle is in the compression zone. With some caution, this phenomenon is analogous to the effect of underloads. It leads to an intensification of damage accumulation.

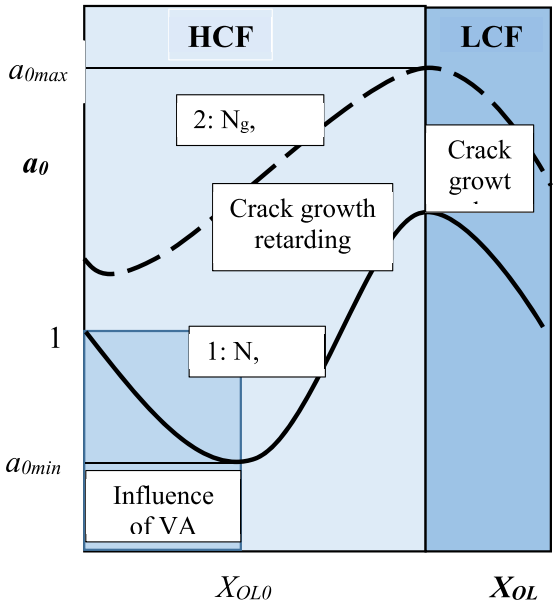

Fig. 3. Overall trends in the behavior of the a_{OL} function.

When the overload level increases $X_{OL} > X_{OL0}$, the crack appears earlier, and the proportion of the endurance period N_g in the total service life *N* increases. In such conditions, the retarding effect of overloads becomes evident, leading to the presence of an ascending branch in the $a_0(X_{OL})$ function (crack growth retarding zone, Fig. 2). Under non-changing sign regimes ($R > 0$), the descending branch degenerates, $X_{OL0} \to 0$ (losing physical meaning), and the $a_0(X_{OL})$ function represents a monotonic ascending branch (2, Fig. 2). The growth of a_0 is restrained by the level of X_{OL}, which corresponds to the yield limit. As mentioned earlier, in such conditions, the retarding effect is lost (crack growth zone, Fig. 2). Conditionally, deformation transitions from the high-cycle fatigue zone (HCF, Fig. 2) to the low-cycle fatigue zone (LCF, Fig. 2), where fracture criteria change.

In semi-logarithmic coordinates a_0 - lgX_{OL} (Fig. 4, a), both branches are expressed by the equations:

$$\left.\begin{array}{l} a_{OL} = p - m_1 \cdot \lg X_{OL} - \text{decreasing branch} \\ a_{OL} = A + m_2 \cdot \lg X_{OL} - \text{ascending branch} \end{array}\right\} \quad (6)$$

It is assumed that to build the model, at least one reliable point a_{0E} is needed, corresponding to the values of X_{OLE}, X_{BE}, R_{OLE}, R_{BE} for the required type of stress-strain state. It is also known to which part (branch) it belongs. The relationships between the parameters of Eq. (6) look like this (Fig. 4, a):

$$\left.\begin{array}{l} m_1 = \dfrac{p - a_{0\,min}}{\Delta_1}, m_2 = \dfrac{a_{0\,max} - a_{0\,min}}{\Delta_2}, \lg X_0 = \dfrac{p - A}{m_1 + m_2}, \\ p = A + (m_1 + m_2) \cdot \lg X_{OLE}, A = a_{0E} - m_2 \cdot \lg X_{OLE}. \end{array}\right\} \quad (7)$$

The parameter *p* corresponds to the stationary loading and should be equal to one. However, this position is true for alternating cycles. For constant cycles, due to hardening, the descending branch intersects the ordinate axis above the point $a_0 = 1$, and it is possible for $p > 1$. When forming a model for steels, it is recommended to take $a_{0min} = 0.5$ (for $R_{OL} < 0$), $a_{0min} = 1.0$ (for $R_{OL} \geq 0$), $\Delta_1 = \Delta_2 = 1$, $X_0 = 5$ ….30, $p = 1$ (for $R_{OL} < 0$), $p = 1.5$ (for $R_{OL} \geq 0$), $m_2 = 0.5$ ….1.5. These parameter values are used in such combinations when there are no experimental values of a_{0E}. Increasing the number of reference points a_{0E} reduces the number of empirically accepted parameters. With one or two values of a_{0E}, according to the recommendations, one or two parameters are accepted,

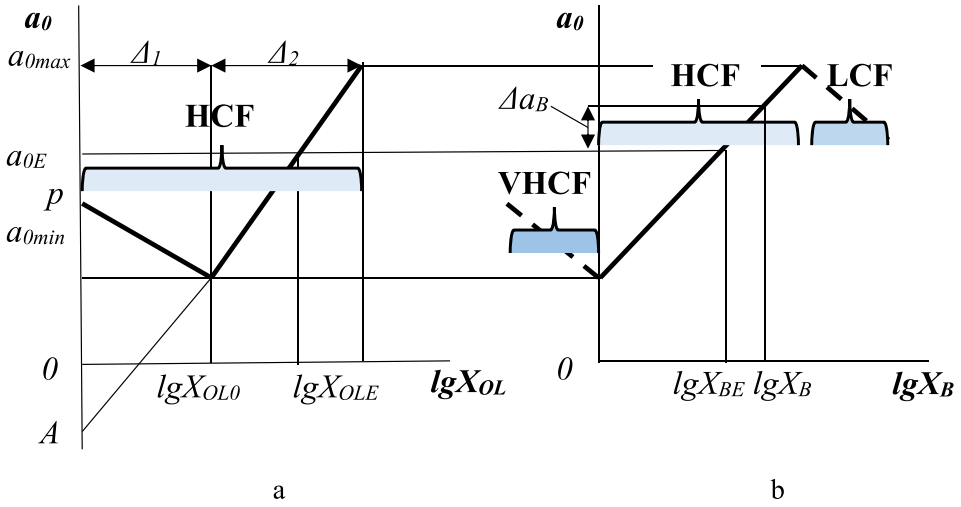

Fig. 4. The basic damage accumulation function a_{OL} (a) and the correction factor from the background level Δa_B (b) in semi-logarithmic coordinates.

and the rest are calculated. Both branches of the a_{OL} function in natural coordinates are combined by the equation:

$$a_{0L} = \lg\left(10^{\mathrm{p}} \cdot X_{\mathrm{OL}}^{-\mathrm{m}_1} \cdot \exp\left(-\frac{X_{\mathrm{OL}}}{X_{\mathrm{OL0}}}\right) + 10^{\mathrm{A}} \cdot X_{\mathrm{OL}}^{\mathrm{m}_2} \cdot \left(1 - \exp\left(-\frac{X_{\mathrm{OL}}}{X_{\mathrm{OL0}}}\right)\right)\right). \tag{8}$$

When the descending branch degenerates, its parameters become $m_1 = 0$, $X_{OL0} \to 0$, and Eq. (8) transforms into Eq. (6).

The influence of the main stage factor (level) B is generally described by a function that has a minimum and a maximum (Fig. 4, b). It is important to know the position of the minimum $a_{0\min}$ on the $a_0(X_{\mathrm{B}})$ curve because X_{B} is measured relative to it. Some researchers believe that the minimum of the $a_0(X_{\mathrm{B}})$ function corresponds to the endurance limit. The increase in a_0 with decreasing X_{B} level (VHCF zone, Fig. 4, b) and the appearance of a minimum can be explained by the weakening interaction between individual load levels. Failure occurs when damage $a_{0\mathrm{i}} = 1$ is reached at one of the levels. Essentially, the damage component solely from overloads reaches one. This part becomes dominant in the overall damage. If this fact is not taken into account, the $a_0(X_{\mathrm{B}})$ curve should theoretically monotonically decrease (Gusev, 1989). To find this minimum, it would be necessary to study in detail the influence of low loads on durability, which was not done within the framework of studying the influence of overloads. As mentioned earlier, $X_{\mathrm{B}} = 1$ is conventionally adopted for elementary damage (Liang et al., 2022). To find this minimum, it is necessary to thoroughly study the influence of low loads on durability, which could not be done within the framework of studying the impact of overloads. As already noted, $X_{\mathrm{B}} = 1$ is conventionally adopted for elementary damage $d_{\mathrm{B}}^{-1} = 10^7$.

To establish a correction for the X_{B} factor in its practically applicable range (VHCF + HCF zone, Fig. 4, b), it is convenient to use semi-logarithmic coordinates.

$$\Delta a_{\mathrm{B}} = m_{\mathrm{B}} \cdot (\lg X_{\mathrm{B}} - \lg X_{\mathrm{BE}}), \tag{9}$$

where $m_{\mathrm{B}} = \frac{a_{0\mathrm{E}} - a_{0\ \min}}{\lg X_{\mathrm{BE}}}$ – slope of the line $a_0(\lg X_{\mathrm{B}})$, usually making up $m_{\mathrm{B}} = 0 \ldots 2$; X_{BE} and X_{B} – damage levels of the primary stage of the process, respectively, the reference (for which the value $a_{0\mathrm{E}}$ is established) and the operating (for which $a_{0\mathrm{i}}$ needs to be found).

If the primary process is in the VHCF range, where $\lg X_{\mathrm{B}} < 0$, then in expression (6), $|\lg X_{\mathrm{B}}|$should be substituted.

3.3.3.1. Cycle asymmetry factor. In the case of alternating cycles, the correction $\Delta a_{0\mathrm{R}}$ consists of two components from the factors $R_{0\mathrm{L}}$ and R_{B} (Fig. 5):

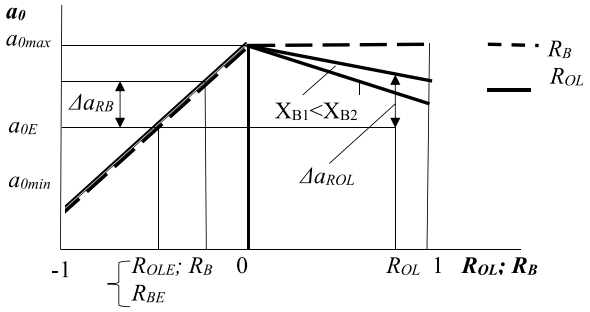

Fig. 5. Diagram illustrating the determination of corrections Δa_{RB} and Δa_{ROL} due to cycle asymmetry.

$$\Delta a_{\mathrm{R}} = m_{\mathrm{ROL}} \cdot (R_{0\mathrm{L}} - R_{0\mathrm{LE}}) + m_{\mathrm{RB}} \cdot (R_{\mathrm{B}} - R_{\mathrm{BE}}), \tag{10}$$

where: m_{ROL} and m_{RB} – slopes of the lines $a_0(R_{0\mathrm{L}})$ and $a_0(R_{\mathrm{B}})$;

$R_{0\mathrm{L}}$ and R_{B} – effective coefficients of overload and base process asymmetry.

Usually $m_{\mathrm{ROL}} = m_{\mathrm{RB}} = 0.5 \ldots 1.0$.In the case of constant-amplitude cycles, the R_{B} factor becomes insignificant (for $R_{\mathrm{B}} > 0$, $m_{\mathrm{RB}} = 0$), and the effect of the $R_{0\mathrm{L}}$ factor starts to depend on the X_B factor. The function $a_0(R)$ becomes decreasing with a slope parameter of m^{+}_{ROL}. This condition is formalized by the following equations (Fig. 5):

$$\left.\begin{aligned} m^{+}_{\mathrm{ROL}} &= 0 \text{ if } 0 < \lg X_{\mathrm{B}} < 1, \\ m^{+}_{\mathrm{ROL}} &= -0.5 m_{\mathrm{R}} (\lg X_{\mathrm{B}} - 1) \text{ if } \lg X_{\mathrm{B}} > 1. \end{aligned}\right\} \tag{11}$$

4. Results and discussion

4.1. The results of software tests

During software loading, characteristic markers remain when transitioning to an overload level, which is absent during steady-state operation (Fig. 6). By counting the number of markers, accurate to one load block, you can determine the durability until the appearance of a crack. Overloads have the main influence on the moment of crack appearance. This can be inferred from the comparison of the fractures in Fig. 6a and b. Despite the nearly twofold difference in durability, the fractures of the samples are identical. This is explained by the fact that sample b (Fig. 6) was previously subjected to steady-state loading at the

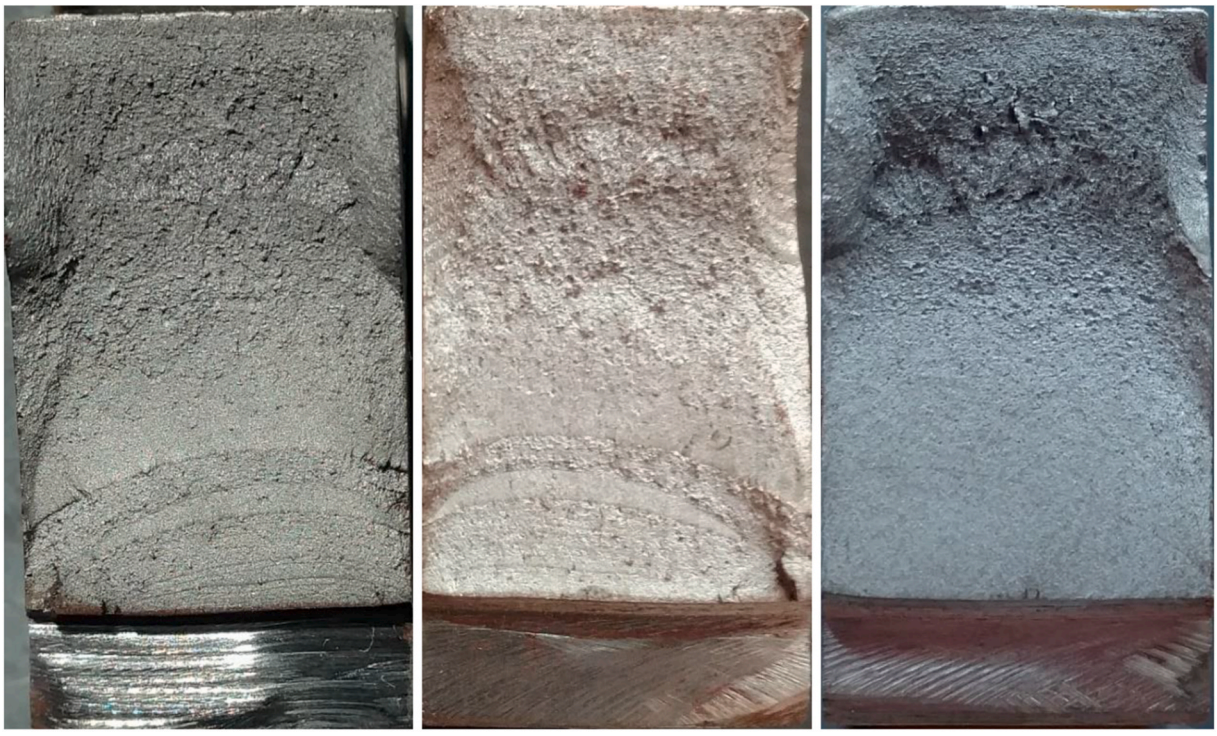

Fig. 6. Fractures of notched specimens made of 35CrMnSi steel (a, b) and 40Cr steel (c), destroyed under programmed loading conditions (a, b) after 420,000 (a), 1,000,000 (b) cycles, as well as under stationary conditions after 1,080,000 cycles.

main level with $X_B \to 1$ for $5{\cdot}10^5$ cycles. There were no significant effects from the loading at this level. After further transitioning to block program loading with increased parameters X_B and X_{OL}, a characteristic fracture pattern was obtained.

The experimentally obtained values of a_{0E} (Table 2) varied within relatively wide limits, indicating the inappropriateness of the LDR for predicting durability and survivability. For steel 40Cr, two options for forming models based on different reference experiments a_{0E} were proposed (Table 3). Then the remaining experiments are considered as validation tests. A comparison of the values of a_0 obtained using the models with experimental ones (Table 2, Fig. 7) confirms the validity of the proposed approach to adjusting accumulated damage.

1. The parameters of the stages are given in terms of relative damages X_{OL} and X_B, as well as in the maximum cycle stresses σ_{OL} and σ_B, calculated as nominal values for bending.
2. Experiments used to obtain Model 1 (*) and Model 2 (**), as reference values for a_{0E}.

The value of a_0 for 35CrMnSi steel is significantly higher than that for 40Cr steel (Fig. 7). Analysis of the fractures provides information that this difference is accompanied by an increase in the number of markers characteristic of the transition to the overload stage. Although 40Cr steel is stronger than 35CrMnSi steel, it has lower fracture toughness and endurance properties. In Belodedenko et al. (2018), it was established using modern methods such as digital image correlation and X-ray diffraction that an increase in strength contributes to a reduction in the retarding effect. The higher the strength, the lower the stress intensity factor of crack initiation, the smaller the size of the plastic zone, and the higher the residual deformation at the crack tip.

It is relevant to comment on the fatigue resistance characteristics of the investigated steels at high values of X_B. For 40Cr steel, there is no increase in the a_0 function with an increase in X_B ($m_B = 0$). This factor becomes less significant. Cracks usually grow at the primary level, and the FCGR serves as an indicator of its level. For 40Cr steel, at the same values of X_B as 35CrMnSi steel, the FCGR on the primary stage will be higher.

At high crack growth rates, overloads cannot slow down the crack growth. From the fracture surfaces, it is evident that in this situation, the crack grows during group overloads. This is also confirmed by the fact that failures on the overload stage occur only at high X_B values, which has been observed in both bending and tension tests (Belodedenko et al., 2006).

This conclusion is consistent with the idea of the absence of a braking effect from decreasing the plasticity of the material (Salvati et al., 2017). Such a situation is observed for steel 40Cr. In addition, high stresses in the main stage can lead to a decrease in favorable residual stresses. Therefore, the influence of overloads at high X_B values decreases (Hesseler et al., 2021).

4.2. Example of applying models in the maintenance of industrial equipment

During the operation of industrial production equipment, there arises the task of planning maintenance actions and the quantity of spare parts needed. This problem arises in the maintenance of the cutting components of mining machinery (miners), for which it is necessary to plan the quantity of cutting tools for replacement (Fig. 8).

In the structure of the mechanical system, cutters belong to the category of tools. These are consumable elements, whose service life is typically determined retrospectively by monitoring their usage. More often than not, cutters wear out due to the wear and tear of their working parts. In such cases, the fatigue strength of the cutting holders has little influence on the operability of the executive mechanism. However, in recent times, the wear resistance of working parts has been significantly improved. Cutters are now more likely to fail within the holders, limiting their operational lifespan. This has raised the issue of finding the optimal material and heat treatment for cutters, as well as predicting their

Table 2
Comparison of the results of block program tests with the results of damage accumulation correction models a_{01} and a_{02}.

# of the experiment	α_σ	σ_B, MPa	σ_{OL}, MPa	X_B	X_{OL}	a_{0E}	a_{0m1}	a_{0m2}
steel 40Cr								
1*	3.5	400	800	100	10	0.6; 1.0; 1.6	1.0	1.4
2*	3.5	270	800	10	100	1.8; 2.4	2.0	2.0
3**	3.5	325	460	27	10	1.2; 1.4; 1.6	1.0	1.4
4	3.5	325	915	27	100	1.9; 2.1	2.0	2.0
5	1.0	955	1315	100	10	0.9; 1.1	1.0	1.4
6	1.0	880	1270	27	10	0.8; 0.9; 1.1	1.0	1.4
7	1.0	880	1315	27	40	1.2; 1.5	1.6	1.8
8	1.0	815	1315	15	70	2.0; 2.3	1.8	1.9
steel 35CrMnSi								
9	3.5	310	390	20	4	2.1; 2.3	2.20	–
10	3.5	400	770	100	10	4.1; 4.2; 4.7	4.27	–
11	3.5	320	530	25	15	3.3; 3.1; 3.5	3.64	–
12	3.5	290	400	10	10	2.4; 2.9; 3.1	2.57	–
13	3.5	310	780	20	60	4.4; 4.8; 5.2	4.8	–

Table 3
Parameters of the accumulated damage correction models.

steel	model	m_1	m_2	X_{OL0}	m_s	p	A
40Cr	1	0	1.0	10	0	1.0	0
40Cr	2	0	0.6	10	0	1.4	0.80
35CrMnSi	1	0	2.2	0	1.7	1	0.88

durability.

For cutters, it is impractical to separate durability into crack initiation and crack propagation stages. Therefore, it is advisable to choose a damage accumulation model. The operating mode of the cutters is similar to the conducted tests: normal cutting processes are interrupted by overloads due to the inclusion of quartzite in coal seams. In this case, in the critical cross-section of the cutting holders, the main process stresses σ_B = 288 MPa act with a coefficient of variation V_B = 0.5. Cutting quartzite leads to an approximately twofold increase in stresses σ_{OL}. Therefore, the relative magnitude of the overload is $OLR = \sigma_{OL}/\sigma_B = 2$. This corresponds to a peak factor value of $\gamma = OLR/V_B = 4$, which can be used to find the relative duration of overload action in a block as (Hesseler et al., 2021; Zhang and Wei, 2022b; Seo et al., 2017):

$$c_{OL} = \exp\left(-\gamma^2/2\right) = 0.00034. \quad (12)$$

Using the equation of the fatigue curve, we determine the damaging parameters of the block stages: $X_B = 10$ and $X_{OL} = 50$ (steel 35CrMnSi); $X_B = 14$ and $X_{OL} = 57$ (steel 40Cr). Based on these values and the obtained models (Table 2), we obtain the maximum accumulated damage values: $a_0 = 1.6$ (steel 35CrMnSi) and $a_0 = 1.8$ (steel 40Cr). Finally, using Eqs. (1) and (2), we find the fatigue life under non-stationary conditions: $N_{VA} = 1.4 \cdot 10^6$ cycles (steel 40Cr) and $N_{VA} = 2 \cdot 10^6$ cycles (steel 35CrMnSi), which correspond to approximately 433 h and 550 h of operation. This means that after these periods, half of the cutters in the mining machine's working body should be replaced.

Considering the significant difference in fatigue and fracture behavior between the two steels discussed, the difference in predicted fatigue life is not very pronounced. This can be explained by the fact that the critical fracture toughness determines the critical crack size. However, for fatigue life, this factor is not as influential as, for example, stress at the primary level.

5. Conclusions

1. Thanks to modeling the loading processes at the damage level d_i in the boundary damage correction models obtained in the research, they are suitable for structural elements with varying degrees of deformation localization. This can be inferred from the fact that the models obtained from notched specimen tests perform satisfactorily under conditions of no localization (un-notched specimens, $\alpha_\sigma = 1$).
2. Based on the generalization of the research results on the resistance of materials to cyclic loading with overloads, a calculation-experimental method for adjusting accumulated damage has been developed and tested under 9 conditions of deformation of alloyed steels with a high-stress gradient at the crack growth stage.

The rate of damage accumulation in overload conditions depends on both the parameters of the loading regime, which affect the shape of the function a_0, and the material properties, which are reflected in the value of a_{0min}.

3. New data on the behavior of the cumulative damage function a_0 under overload conditions have been obtained. It was previously believed that when transitioning to constant load cycles, the a_0 function becomes smoother and less sensitive to loading parameters. However, under the investigated deformation conditions, the value of a_0 varies widely, ranging from 0.5 to 4.7.

At high levels of damage in the primary overload stage, even positive cycle asymmetry cannot slow down the damage process. Therefore, there are conditions that contribute to the relative reduction of the a_0 magnitude in stress localization zones. This should be kept in mind if maintenance personnel decide to extend the durability of a structure by artificially creating "braking" overloads.

4. During the crack growth stage, overloads can increase the durability by 1–2 orders of magnitude, which leads to a significant increase in accumulated damage. The developed algorithm allows for the prediction of durability without separating it into crack initiation and propagation stages. When assessing the resource based on damage accumulation, the hidden period of durability in stress localization zones significantly affects the calculation results, which is particularly characteristic of components made of strong steel where cracks are hard to detect.

CRediT authorship contribution statement

S. Belodedenko: Supervision, Conceptualization. **O. Hrechanyi:** Resources, Project administration, Methodology. **V. Hanush:** Writing – original draft, Data curation. **Y. Izhevskyi:** Writing – review & editing.

Declaration of competing interest

The authors declare that they have no known competing financial interests or personal relationships that could have appeared to influence the work reported in this paper.

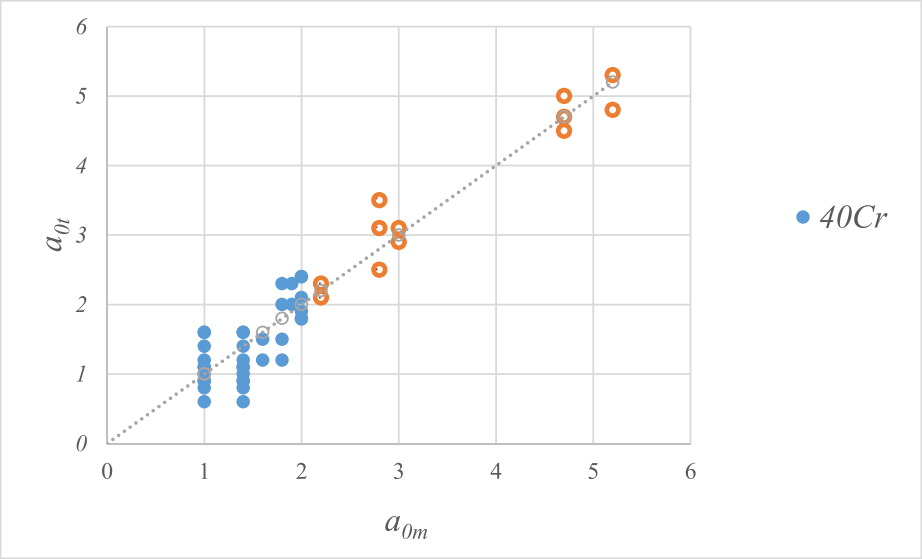

Fig. 7. Comparison of experimental values of a_{ot} with calculated a_{0m} for notched and unnotched samples (the dashed line shows the line of perfect correspondence).

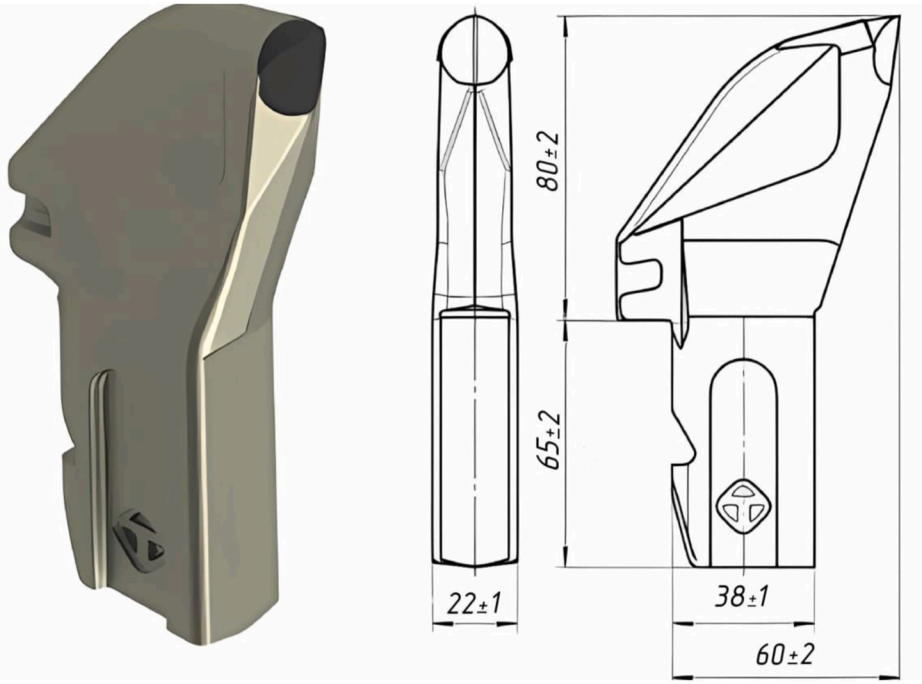

Fig. 8. Radial cutters of the mining tool plant (Dnipro, Ukraine) for coal miners.

Data availability

Data will be made available on request.

References

Abdullah, S., Choi, J.C., Yiacomin, J.A., Yates, J.R., 2006. Bump extraction algorithm for variable amplitude fatigue loading. Int. J. Fatig. (7), 675–691. https://doi.org/10.1016/j.ijfatigue.2005.09.003.

Będkowski, W., 2014. Assessment of the fatigue life of machine components under service loading a review of selected problems. J. Theor. Appl. Mech. 52 (2), 443–458.

Belodedenko, S.V., 2003. Research and forecasting of the distribution of durability under cyclic loading with overloading. Zavodsk. Lab. Diag. Mater. 69 (3), 43–47.

Belodedenko, S.V., 2005. Estimation of safe longevity of construction under design and exploitation of equipment. Zavodsk. Lab. Diagn. Mater. 6, 40–46.

Belodedenko, S.V., 2010. Forecasting the survivability of technological equipment elements using damage accumulation models. Zavodsk. Lab. Diagn. Mater. 76 (1), 49–52.

Belodedenko, S.V., Bilichenko, G.N., Kozakov, D.E., 1997. Accumulation of fatigue damage and lifetime prediction under irregular loading conditions with overloads and random cycle asymmetry. Strength Mater. 29 (2), 137–141. https://doi.org/10.1007/bf02767589.

Belodedenko, S.V., Bilichenko, G.N., Ermokrattev, V.A., 2006. Investigation of the influence of the increase in cycle asymmetry and overloads on damage accumulation in high-strength steel. In: У Mechanical fatigue of Metals: Proceeding of the 13-th Int. colloquium, pp. 145–151.

Belodedenko, S., Grechany, A., Ibragimov, M., 2018. Risk indicators and diagnostic models for sudden failures. Sci. J. Ternopil Nat. Tech. Univ. 88 (4), 111–118. https://doi.org/10.33108/visnyk_tntu2017.04.111.

Belodedenko, S., Hanush, V., Baglay, A., Hrechanyi, O., 2020. Fatigue resistance models of structural for risk based inspection. Civil Eng. J. 6 (2), 375–383. https://doi.org/10.28991/cej-2020-03091477.

Belodedenko, S.V., Hanush, V.I., Hrechanyi, O.M., 2022. Experimental verification of the survivability model under mixed I+II mode fracture for steels of rolling rolls. Struct. Integr. 25, 3–12. https://doi.org/10.1007/978-3-030-91847-7_1.
Belodedenko, S., Hrechanyi, O., Vasilchenko, T., Hrechana, A., Izhevskyi, Y., 2023. Determination of the critical cyclic fracture toughness for the II mode in mixed fracture of structural steels. Forces Mech. 13, 100236 https://doi.org/10.1016/j.finmec.2023.100236.
Bleicher, C., Wagener, R., Kaufmann, H., 2019. Fatigue behavior of large cast components under variable amplitude loading with overloads. In: WCX SAE World Congress Experience. 400 Commonwealth Drive, Warrendale, PA, United States. https://doi.org/10.4271/2019-01-0526.
Borrego, L.P., Costa, J.M., Ferreira, J.M., 2005. Fatigue crack growth in thin aluminium alloy sheets under loading sequences with periodic overloads. Thin-Walled Struct. 43 (5), 772–788. https://doi.org/10.1016/j.tws.2004.11.001.
Cai, L., Li, W., Hu, T., Ji, B., Zhang, Y., Sakai, T., Wang, P., 2022. In-situ experimental investigation and prediction of fatigue crack growth for aluminum alloys under single spike-overloads. Eng. Fract. Mech. 260, 108195 https://doi.org/10.1016/j.engfracmech.2021.108195.
Chan, Wing, Wang, A., Shoup, J.M., 1999. Real time torque measurement of rolling mill drive. In: Conference Record of the 1999 IEEE Industry Applications Conference. Thirty-Forth IAS Annual Meeting (Cat. No.99CH36370), Phoenix, AZ, USA, pp. 557–564. https://doi.org/10.1109/IAS.1999.800007, 1.
Collacott, R.A., 1985. Structural Integrity Monitoring. Chapman and Hall.
Dawicke, D.S., 1997. Overload and Underload Effects on the Fatigue Crack Growth Behavior of the 2024-T3 Aluminum Alloy (No. NAS 1.26: 201668).
Ding, Z., Wang, X., Gao, Z., Bao, S., 2017. An experimental investigation and prediction of fatigue crack growth under overload/underload in Q345R steel. Int. J. Fatig. 98, 155–166. https://doi.org/10.1016/j.ijfatigue.2017.01.024.
Duan, H., He, H., Yue, S., Cao, M., Zhao, Y., Zhang, Z., Liu, Y., 2023. Analysis of High-cycle fatigue life prediction of 304 stainless steel based on deep learning. JOM. https://doi.org/10.1007/s11837-023-06042-8.
Fatemi, A., Yang, L., 1998. Cumulative fatigue damage and life prediction theories: a survey of the state of the art for homogeneous materials. Int. J. Fatig. 20 (1), 9–34. https://doi.org/10.1016/s0142-1123(97)00081-9.
Field, I., Kandare, E., Dixon, B., Tian, J., Barter, S., 2022. Effect of underloads in small fatigue crack growth. Int. J. Fatig. 157, 106706 https://doi.org/10.1016/j.ijfatigue.2021.106706.
Fleck, N.A., 1985. Fatigue crack growth due to periodic underloads and overloads. Acta Metall. 33 (7), 1339–1354. https://doi.org/10.1016/0001-6160(85)90244-5.
Fomichev, P.A., 2006. Energy-based approach to lifetime calculation under random loading. In: Mechanical Fatigue of Metals: Proceeding of the 13-th Int. Colloquium, Ternopil: TSTU, pp. 119–128.
Gadallah, R., Murakawa, H., Shibahara, M., 2023. Thickness and weld orientation effects on fatigue crack growth after a single tensile overload. Int. J. Pres. Ves. Pip., 105020 https://doi.org/10.1016/j.ijpvp.2023.105020.
Garcia, E., Montés, N., Llopis, J., Lacasa, A., 2022. Miniterm, a novel virtual sensor for predictive maintenance for the Industry 4.0 era. Sensors (22), 6222. https://doi.org/10.3390/s22166222.
Gusev, A.S., 1989. Fatigue Resistance and Survivability of Structures under Random Loads. Mashinostroenie (in Russian).
Hectors, K., De Waele, W., 2021. Cumulative damage and life prediction models for high-cycle fatigue of metals: a review. Metals 11 (2), 204. https://doi.org/10.3390/met11020204.
Hesseler, J., Baumgartner, J., Bleicher, C., 2021. Consideration of the transient material behavior under variable amplitude loading in the fatigue assessment of nodular cast iron using the strain-life approach. Fatig. Fract. Eng. Mater. Struct. 44 (10), 2845–2857. https://doi.org/10.1111/ffe.13519.
Jones, R.E., 1973. Fatigue crack growth retardation after single-cycle peak overload in Ti-6Al-4V titanium alloy. Eng. Fract. Mech. 5 (3), 585–588. https://doi.org/10.1016/0013-7944(73)90042-8.
Krot, P., Prykhodko, I., Raznosilin, V., Zimroz, R., 2020. Model based monitoring of dynamic loads and remaining useful life prediction in rolling mills and heavy machinery. In: Ⅴ Advances in Asset Management and Condition Monitoring. Springer International Publishing, pp. 399–416. https://doi.org/10.1007/978-3-030-57745-2_34.
Laseure, N., Schepens, I., Micone, N., De Waele, W., 2015. Effects of variable amplitude loading on fatigue life. Int. J. Spray Combust. Dyn. 6 (3), 10. https://doi.org/10.21825/scad.v6i3.1131.
Lee, D., Kwon, H.-J., Choi, K., 2022. Risk-based maintenance optimization of aircraft gas turbine engine component. Proc. Inst. Mech. Eng. O J. Risk Reliab. https://doi.org/10.1177/1748006X221135907.
Liang, H., Zhan, R., Wang, D., Deng, C., Guo, B., Xu, X., 2022. Fatigue crack growth under overload/underload in different strength structural steels. J. Constr. Steel Res. 192, 107213 https://doi.org/10.1016/j.jcsr.2022.107213.
Lin, J., Li, W., Yang, S., Zhang, J., 2018. Vibration fatigue damage accumulation of Ti–6Al–4V under constant and sequenced variable loading conditions. Metals 8 (5), 296. https://doi.org/10.3390/met8050296.
Liu, Y., Mahadevan, S., 2007. Stochastic fatigue damage modeling under variable amplitude loading. Int. J. Fatig. 29 (6), 1149–1161. https://doi.org/10.1016/j.ijfatigue.2006.09.009.
Miner, M.A., 1945. Cumulative damage in fatigue. J. Appl. Mech. 12 (3), 159–164.
Neto, D.M., Sérgio, E.R., Borges, M.F., Borrego, L.P., Antunes, F.V., 2022. Effect of load blocks on fatigue crack growth. Int. J. Fatig. 162, 107001 https://doi.org/10.1016/j.ijfatigue.2022.107001.
Nottebaere, T., Micone, N., De Waele, W., 2017. A comparison of fatigue lifetime prediction models applied to variable amplitude loading. Int. J. Spray Combust. Dyn. 8 (1) https://doi.org/10.21825/scad.v8i1.6809.
Peng, Z., Huang, H.-Z., Wang, H.-K., Zhu, S.-P., Lv, Z., 2015. A new approach to the investigation of load interaction effects and its application in residual fatigue life prediction. Int. J. Damage Mech. 25 (5), 672–690. https://doi.org/10.1177/1056789515620910.
Pereira, M.V.S., Darwish, F.A.I., Camarão, A.F., Motta, S.H., 2007. On the prediction of fatigue crack retardation using Wheeler and Willenborg models. Mater. Res. 10 (2), 101–107. https://doi.org/10.1590/s1516-14392007000200002.
Phillips, E.P., 1999. Periodic Overload and Transport Spectrum Fatigue Crack Growth Tests of Ti62222STA and Al2024T3 Sheet. National Aeronautics and Space Administration, Langley Research Center.
Rege, K., Grønsund, J., Pavlou, D.G., 2019. Mixed-mode I and II fatigue crack growth retardation due to overload: an experimental study. Int. J. Fatig. 129, 105227 https://doi.org/10.1016/j.ijfatigue.2019.105227.
Rice, R.C., Stephens, R.I., 1973. Overload effects on subcritical crack growth in austenitic manganese steel. ASTM STP 536, 95–114.
Salvati, E., Zhang, H., Fong, K.S., Song, X., Korsunsky, A.M., 2017. Separating plasticity-induced closure and residual stress contributions to fatigue crack retardation following an overload. J. Mech. Phys. Solid. 98, 222–235. https://doi.org/10.1016/j.jmps.2016.10.001.
Santecchia, E., Hamouda, A.M.S., Musharavati, F., Zalnezha, E., Cabibbo, M., El Mehtedi, M., Spigarelli, S., 2016. A review on fatigue life prediction methods for metals. Adv. Mater. Sci. Eng. 1–26. https://doi.org/10.1155/2016/9573524.
Seo, S., Huang, E.-W., Woo, W., Lee, S.Y., 2017. Neutron diffraction residual stress analysis during fatigue crack growth retardation of stainless steel. Int. J. Fatig. 104, 408–415. https://doi.org/10.1016/j.ijfatigue.2017.08.007.
Shakeri, I., Shahani, A.R., Rans, C.D., 2021. Fatigue crack growth of butt welded joints subjected to mixed mode loading and overloading. Eng. Fract. Mech. 241, 107376 https://doi.org/10.1016/j.engfracmech.2020.107376.
Shlyushenkov, A.P., Tatarintsev, V.A., 1994. Fatigue damage accumulation in steel 45 on loading involving few-cycle overloading. Strength Mater. 26 (5), 337–341. https://doi.org/10.1007/bf02207416.
Song, S.H., Lee, K.R., Kim, A., 2001. Analysis on short crack growth rate after single overload under cyclic bending moment. Int. J. Precis. Eng. Manuf. 2 (3), 19–26.
Sonsino, C.M., Kau Fmann, H., Wagener, R., Fischer, C., Eufinger, J., 2011. Interpretation of overload effects under spectrum loading of welded high-strength steel joints. Weld. World 55 (11–12), 66–78. https://doi.org/10.1007/bf03321544.
Sousa, F.C., Akhavan-Safar, A., da Silva, L.F.M., 2022. Single and periodic overloading effects on the mode I fatigue crack growth of a ductile adhesive. Theor. Appl. Fract. Mech. 121, 103528 https://doi.org/10.1016/j.tafmec.2022.103528.
Tipton, S.M., Sorem, J.R., 1999. Fatigue durability enhancement by controlled overloading. In: Panontin, T.L., Sheppard, S.D. (Eds.), Fatigue and Fracture Mechanics: 29th Volume. ASTM International, West Conshohocken, PA.
Xie, L.-q., Zhou, C.-y., Zhang, P., He, X.-h., 2022. Fatigue crack growth under mixed mode I-II loading with a single tensile overload at negative load ratios. Theor. Appl. Fract. Mech. 118, 103294 https://doi.org/10.1016/j.tafmec.2022.103294.
Zhang, L., Wei, X., 2022a. Prediction of fatigue crack growth under variable amplitude loading by artificial neural network-based Lagrange interpolation. Mech. Mater., 104309 https://doi.org/10.1016/j.mechmat.2022.104309.
Zhang, L., Wei, X., 2022b. Prediction of fatigue crack growth under variable amplitude loading by artificial neural network-based Lagrange interpolation. Mech. Mater. 171, 104309 https://doi.org/10.1016/j.mechmat.2022.104309.
Zhang, H., Ray, A., Patankar, R., 1998. Damage-mitigating control with overload injection: experimental validation of the Concept 1. J. Dyn. Syst. Meas. Control 122 (2), 336–342. https://doi.org/10.1115/1.482460.
Zhou, X., Hohenwarter, A., Leitner, T., Gänser, H.P., Pippan, R., 2015. Load history effects on fatigue crack propagation: its effect on the R-curve for threshold. Frat. Ed. Integrità Strutt. 9 (33), 209–214. https://doi.org/10.3221/igf-esis.33.26.